RAA 2015 Vol. **15** No. **10**, 1758–1772 doi: 10.1088/1674–4527/15/10/013
http://www.raa-journal.org *http://www.iop.org/journals/raa*

Research in Astronomy and Astrophysics

Studying solutions for the fatigue of the FAST cable-net structure caused by the process of changing shape

Peng Jiang[1,2], Ren-Dong Nan[1,2], Lei Qian[1,2] and You-Ling Yue[1,2]

[1] National Astronomical Observatories, Chinese Academy of Sciences, Beijing 100012, China; *pjiang@bao.ac.cn*
[2] Key Laboratory of Radio Astronomy, Beijing 100012, China

Received 2015 January 2; accepted 2015 April 10

Abstract The Five-hundred-meter Aperture Spherical Radio Telescope (FAST) is supported by a cable-net structure, whose change in shape leads to a stress range of approximately 500 MPa. This stress range is more than twice the standard recommended value. The cable-net structure is thus the most critical and fragile part of the FAST reflector system. In this study, we first search for a more appropriate deformation strategy that reduces the stress amplitude generated by the process of changing shape. Second, we roughly estimate the tracking trajectory of the telescope during its service life, and conduct an extensive numerical investigation to assess the requirements for fatigue resistance. Finally, we develop a new type of steel cable system that satisfies the cable requirements for construction of FAST.

Key words: five-hundred-meter aperture spherical radio telescope — fatigue resistance — astronomical techniques and approaches — cable-net structure — finite element

1 INTRODUCTION

The Five-hundred-meter Aperture Spherical Radio Telescope (abbreviated as FAST), one of the key scientific projects that was part of China's 11th Five-year Plan, was approved for construction by the National Development and Reform Commission on 2007 July 10. FAST will make observations at frequencies from 70 MHz to 3 GHz. The design resolution and pointing accuracy will be $2.9'$ and $8''$ respectively. To achieve these technical specifications, the root-mean-square value of the out-of-plane error of the reflector should be no more than 5 mm (Nan et al. 2003, 2011).

According to the principle of geometrical optics used by FAST (illustrated in Fig. 1), the supporting structure of the reflector system should be capable of forming a parabolic surface from a spherical surface. This is the most prominent special requirement of the telescope beyond those of conventional structures. Staff at the National Astronomy Observatories, Chinese Academy of Sciences, have been carrying out a rigorous feasibility study of critical technologies since 1994. More than 100 scientists and engineers from 20 institutions have been involved in the project. An extensive comparative analysis of several design plans for the supporting structure of the reflector system was performed (Luo et al. 2004; Lu & Ren 2007). An Arecibo-type plan was selected because a cable-net structure can easily accommodate the complex topography of Karst terrain, thus

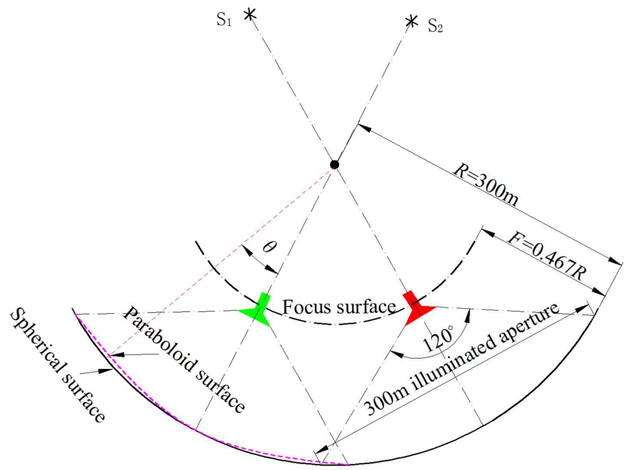

Fig. 1 The principle of geometrical optics used by FAST.

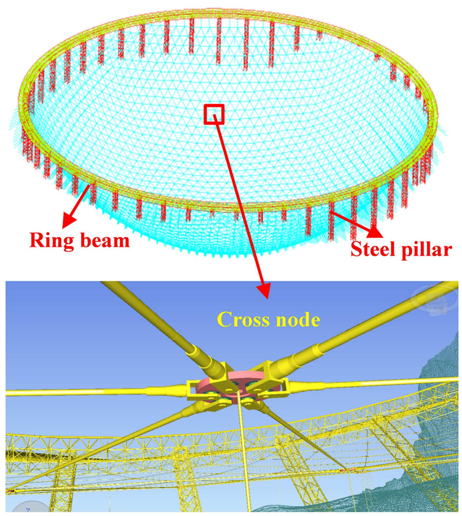

Fig. 2 Concept of the adaptive cable-net structure.

avoiding the need to construct heavy civil engineering works between actuators and the ground (see Fig. 2) (Qian et al. 2005).

Later, an extensive numerical comparative analysis was performed among several different cell types, such as three-dimensional cells, Kiewitt cells and geodesic triangular cells. Geodesic triangular cells were selected because their stress distribution is more even (Qian et al. 2005; Jiang et al. 2013).

The cable net is comprised of 6670 steel cables and approximately 2225 cross nodes. The lengths of cables range from 10.5 to 12.5 m, the total weight of the net is 1300 tons, and the cross sections of the main cables have 16 different areas ranging from 280 to 1319 mm^2. None of the cables are connected, allowing us to set their cross sections according to their loads.

The outer edge of the cable net is suspended from a steel ring beam whose diameter is 500 m (see Fig. 2). The cross nodes of the cable net are used as control points. Each cross node is connected to an actuator by a down-tied cable. By controlling the actuator using feedback from the measurement and control system, the positions of the cross nodes can be adjusted to form an illuminated aperture having a diameter up to 300 m. This illuminated aperture moves along the spherical surface according to the zenith angle of the target objects (see S_1 and S_2 in Fig. 1).

The above description clearly indicates that long-term observations by FAST will lead to the long-term and frequent process of changing shape in the cable-net structure. Previous research has shown that such a process of changing shape introduces a stress range on the order of 500 MPa, which is nearly twice the standard recommended value.[1,2,3] The cable-net structure is thus the most critical and fragile part of the FAST reflector system.

To improve the reliability and service life of FAST, the present work, on the basis of the final design, searches for a way to reduce the stress range acting on the cable during the process of changing shape and develops a new type of cable system with ultra high fatigue resistance that meets the requirements for operating FAST.

In Section 2, theoretical and numerical methods are used to search for a more appropriate deformation strategy that reduces the stress amplitude generated by the process of changing shape. Furthermore, we roughly estimate the tracking trajectory of the telescope during its service life, and conduct an extensive numerical investigation to assess the requirements for fatigue resistance. In Section 3, extensive experiments have been performed on different types of coating strands, and a detailed design of the anchor system has been investigated. Finally, we develop a new type of steel cable system that satisfies the cable requirements for construction of FAST.

2 OPTIMIZATION OF THE DEFORMATION STRATEGY

2.1 Analysis of the Main Influencing Factors

In general, the illuminated aperture is a parabolic surface, whose profile can be expressed as

$$x^2 = 2py + c\,. \tag{1}$$

The variables and parameters of the problem are the weight of the reflector element w, the density of the cable ρ, the elastic modulus of the cable E, the cross-sectional area of the cable A_i, the geometric parameters of the illuminated aperture p and c, the diameter of the illuminated aperture d, the radius of the cable-net structure R, and the diameter of the ring beam D. The stress amplitude can thus be expressed as

$$\Delta\sigma = f(w, E, \rho, A_i, p, c, D, d, R)\,. \tag{2}$$

Among these governing parameters, E, d and ρ have independent dimensions. By applying the Buckingham-Pi theorem from dimensional analysis (Barenblatt 1996), we obtain

$$\frac{\Delta\sigma}{E} = \prod\left(\frac{w}{\rho d}, \frac{A_i}{d^2}, \frac{p}{d}, \frac{c}{d^2}, \frac{D}{d}, \frac{R}{d}\right)\,. \tag{3}$$

In our final design, w, d, R, D and A_i are already determined; the weight of the reflector element w is approximately 17 $\mathrm{kg\ m^{-2}}$, the diameter of the illuminated aperture d is 300 m, the radius of the cable-net R is 300 m, the diameter of the ring beam D is 500 m, and all cross sections of the cable

[1] ISO15630-3 2002, Steel for Reinforcement and Pre-stressing of Concrete Test Methods – Part 3: Pre-stressing Steel, Int. Org. for Standardization, Int. Org. for Standardization

[2] Post-Tensioning Institute 2001, Recommendations for stay cable design, testing and installation, PTI, Phoenix

[3] Federation International du Beton 2003, Recommendations for the acceptance of stay cable systems using prestressing steels, FIB, Lausanne.

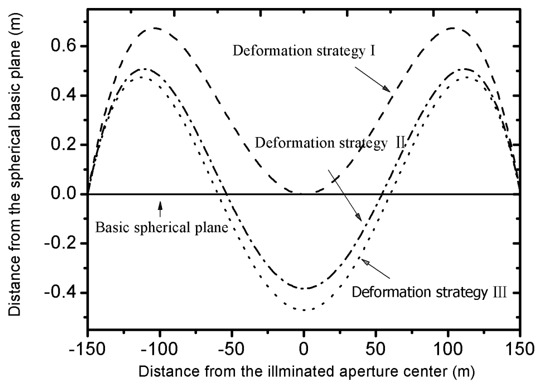

Fig. 3 Relative positions of the parabolic surface and the basic spherical surface in three previously proposed deformation strategies.

A_i have been determined according their loads. For a steel cable, ρ is approximately $7850\ \mathrm{kg\ m^{-3}}$. Thus, Equation (2) can be simplified as

$$\frac{\Delta\sigma}{E} = \prod\left(\frac{p}{d}, \frac{c}{d^2}\right). \quad (4)$$

Furthermore, the nodes of the outer edge of the cable net are fixed to the ring beam and, in contrast to the case for the other cross nodes, their positions cannot be adjusted by the actuator. To expand the observation zenith angle as much as possible, the outer edge of the illuminated aperture should coincide with the basic spherical surface. Only then can the outer edge of the illuminated aperture arrive at the outer edge of the cable net. Under such a constraint, we can derive that

$$c = 22500 + 2p\sqrt{67500}. \quad (5)$$

Equation (3) can then be further simplified as

$$\frac{\Delta\sigma}{E} = \prod\left(\frac{p}{d}\right). \quad (6)$$

The elastic modulus of steel cable is about 200 GPa, and thus the only variable remaining in the implicit function of Equation (6) is p/d, which is the focal ratio of the telescope.

From Equation (6) we know that the fatigue stress range of a cable used by FAST is most dependent on the focal ratio of the telescope. A different focal ratio would lead to a different relative position between the illuminated aperture and the basic plane, which is directly related to internal forces of the cable net and stroke of the actuator.

In our earlier work (Jiang et al. 2013), we proposed three deformation strategies, namely strategies I, II and III. The relative positions of the illuminated aperture with respect to the spherical basic plane in these three strategies are shown in Figure 3.

Among these strategies, strategies I and II respectively have the shortest actuator stroke and the minimum peak distance from the illuminated aperture to the basic spherical surface. The actuator stroke is approximately 0.67 m in strategy I and the maximum deviation is approximately 0.47 m in strategy II. Strategy III is based on the principle of equal arclengths; i.e., the profile arclength of the illuminated aperture is equal to that of the spherical basic plane. The focal ratios corresponding to these three strategies are respectively 0.4665, 0.4611 and 0.4613.

In the preliminary design of the FAST cable-net structure, deformation strategy I was recommended as the preferred control scheme simply because it has the shortest actuator stroke. Obviously, it is unreasonable to omit the fatigue problem in the optimization of the deformation strategy, especially in the present case where stress range is of the order of 500 MPa.

The present work thus establishes a relation between the focal ratio and deformation stress range. By considering both the actuator stroke and stress range of the cable, we can reconsider our recommended deformation strategy for FAST observations.

2.2 Simplified Analysis Method

We use ANSYS software to build a finite element model of the entire supporting structure, which is comprised of a cable net, down-tied cable, ring beam and steel pillar (see Fig. 2). Link10 elements and beam 188 elements are respectively used to simulate the response of the cable-net structure and the steel ring beam structure.

When not in operation, the FAST cable net should hold a spherical shape under the combined loads of gravity, initial stress, and the down-tied cable. To derive such a state, inverse iteration is applied. When FAST is making observations, the deformation procedure for forming the illuminated aperture from the spherical shape can be simulated by employing a conventional iteration method.

According to the working principle of FAST, the motion of the cable net cross nodes during the process of changing shape is very slow. If we define the center of the sphere as the origin of coordinates and take the observation direction as the polar axis, the polar equation of the illuminated aperture can be expressed as

$$\sin^2\theta \cdot \rho^2 - 553.294 \cdot \cos\theta \cdot \rho - 166250 = 0\,, \tag{7}$$

where ρ is the distance from the cross node to the center of the sphere and θ is the polar angle of the cross node (see Fig. 1).

In the process of changing shape, the tangential displacement of the cross node is negligibly small. The velocity and acceleration of the cross node can then be expressed as

$$\begin{cases} v(\theta) = \frac{d\rho}{d\theta} \cdot \frac{d\theta}{dt}\,, \\ a(\theta) = \frac{d\left(\frac{d\rho}{d\theta} \cdot \frac{d\theta}{dt}\right)}{d\theta} \cdot \frac{d\theta}{dt}\,. \end{cases} \tag{8}$$

The tracking angular velocity of FAST is 15 degrees per hour. Substituting the angular velocity into Equation (8), we find that the maximum speed of the cross node is no more than 0.58 mm s^{-1}. Thus, the process of changing shape for the FAST cable net is approximated here as a quasi-static process.

According to the operating principle used by FAST, the illuminated aperture center is restricted within a certain region as shown in Figure 4. This region contains 550 cross nodes, with the interval between any two adjacent nodes being no more than 12.5 m, which approximately corresponds to a central angle of only 1 degree for the 300-m-radius reflector; this interval is much smaller than the illuminated aperture.

We assume that the distribution of the 550 discrete points is sufficiently dense, and any possible observation state is approximately equivalent to one of the 550 deformation states whose illuminated aperture centers correspond to these 550 cross nodes. The peak stress range of each cable can then be easily derived from simulation results for the 550 deformation states.

To verify whether the distribution of discrete points is sufficiently dense, comparative analysis was performed for deformation strategy II using the above mentioned 550 discrete points and a denser distribution of discrete points. In the latter case, the discrete points not only include the cross nodes but also the mid-point of each cable and the middle of each triangular element; thus, more than 2200 deformation states need to be simulated for the one deformation strategy.

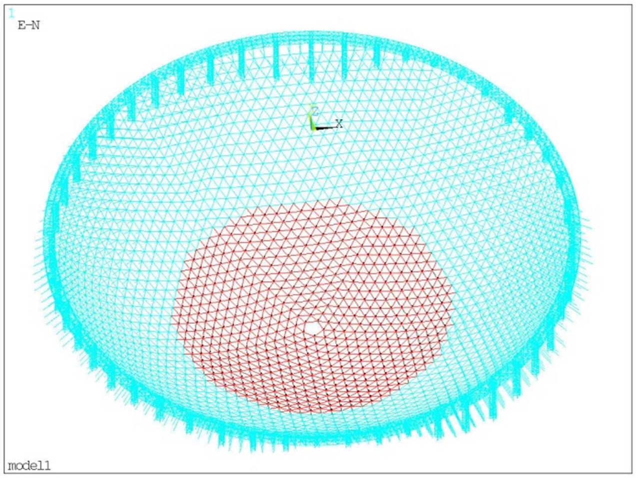

Fig. 4 Illustration of cross nodes used as discrete points to describe the continuous trajectory path of the illuminated aperture center.

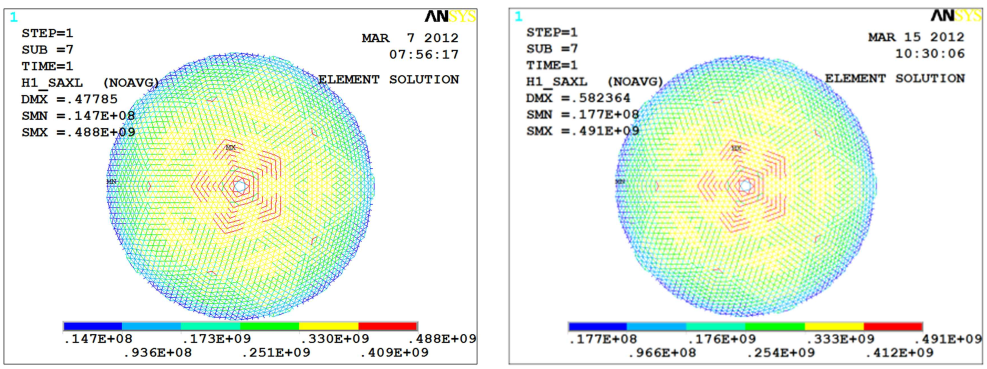

(a) (b)

Fig. 5 Comparison of the simulation results of deformation strategy II obtained using 550 and 2200 discrete points. (a) Result obtained using 550 discrete points. (b) Result obtained using 2200 discrete points.

The calculation results derived using the two sets of discrete points described above are shown in Figure 5(a) and (b). The peak stress ranges derived using 550 and 2200 discrete points are respectively 488 and 491 MPa, with a difference of less than 1%. We thus assume that using 550 cross nodes provides sufficient accuracy in our case. The subsequent work in this paper is based on this assumption.

2.3 Analysis Results

Employing the same procedure used in the previous section, the peak stress range generated by several deformation strategies with different focal ratios can be derived (see Table 1). The peak stress

Table 1 Comparison of the fatigue stress range of the cable and the stroke of the actuator when employing different deformation strategies.

Focal ratio	0.4603	0.4611	0.4613	0.4620	**0.4621**	0.4622	0.4633	0.4665
Maximum stress range (MPa)	512	488	482	462	**455**	460	488	547
Actuator stroke (m)	0.9890	0.9450	0.9341	0.8966	**0.8914**	0.8861	0.8291	0.6741

range, taken as an analytical factor, is obtained for different focal ratios. The simulation results reveal that the stress range has a minimum value of 455 MPa when the focal ratio is 0.4621.

To verify that the optimum focal ratio is 0.4621 for the fatigue problem of the cable net, focal ratios of 0.4620 and 0.4622 were also investigated. The simulation showed that the peak stress ranges when employing these two deformation strategies are respectively 462 and 460 MPa. Both of these are slightly higher than what results when employing the deformation strategy with a focal ratio of 0.4621. Therefore, we have reason to believe that the deformation strategy with a focal ratio of 0.4621 is very close to the optimum deformation strategy having the minimum stress range.

It should also be noted that the actuator stroke in the strategy is 0.89 m, which is 50 mm less than that in strategy II. By comparing the stress range and actuator stroke of the deformation strategies (see Table 1), we recommend a strategy with a focal ratio of 0.4621 for application to FAST.

3 ASSESSMENT OF FATIGUE RESISTANCE

According to the working principle of FAST, the problem of fatigue in the cable-net structure arises from the process of changing shape. The stress-time history of the cable would directly depend on the trajectory of the illuminated aperture. Therefore, the present work on the assessment of fatigue in the cable net structure can be divided into several parts.

First, according to the scientific goal and observation model of the telescope, we roughly plan the trajectory of the illuminated aperture for a service life of the telescope that is 30 years.

Second, employing a simplified finite element method, the stress-time history curve of each cable is derived from the trajectory of the illuminated aperture.

Finally, using a reasonable mathematical statistical method to deal with the stress-time history curve of the cable, we can count the approximate number of fatigue cycles for each cable.

3.1 Planning the Observation Trajectory

Regarding the scientific goals of FAST, types of observations made with the telescope can be divided into five classes: pulsars, neutral hydrogen, molecular spectral lines, very-long-baseline interferometry and the search for extraterrestrial intelligence. The observing mode can then also be divided into three types: pulsar searching and monitoring, neutral-hydrogen large-area and small-area scanning, and other observations. We assume that each of these three types of observations accounts for one-third of the observation time.

According to unofficial statistics for the first half of 2009, the observation uptime of the Green Bank Radio Telescope was approximately 70% to 80%, and the uptime of the Xinjiang 25-meter radio telescope was approximately 74%. Considering the complexity of systems associated with FAST, more maintenance time will probably be needed for FAST. It is thus reasonable to assume that the FAST uptime will be no more than 70%.

Making the above assumption and employing the principle of randomization, we can roughly plan the trajectory of the illuminated aperture during the service life of the telescope. A trajectory data file is then created. The data include a total of 228 715 observations and 3 410 008 tracking points. The interval of time between tracking points is 120 seconds, and the corresponding spherical solid angle at the surface of the reflection is about 0.5 degrees. In employing the trajectory of the

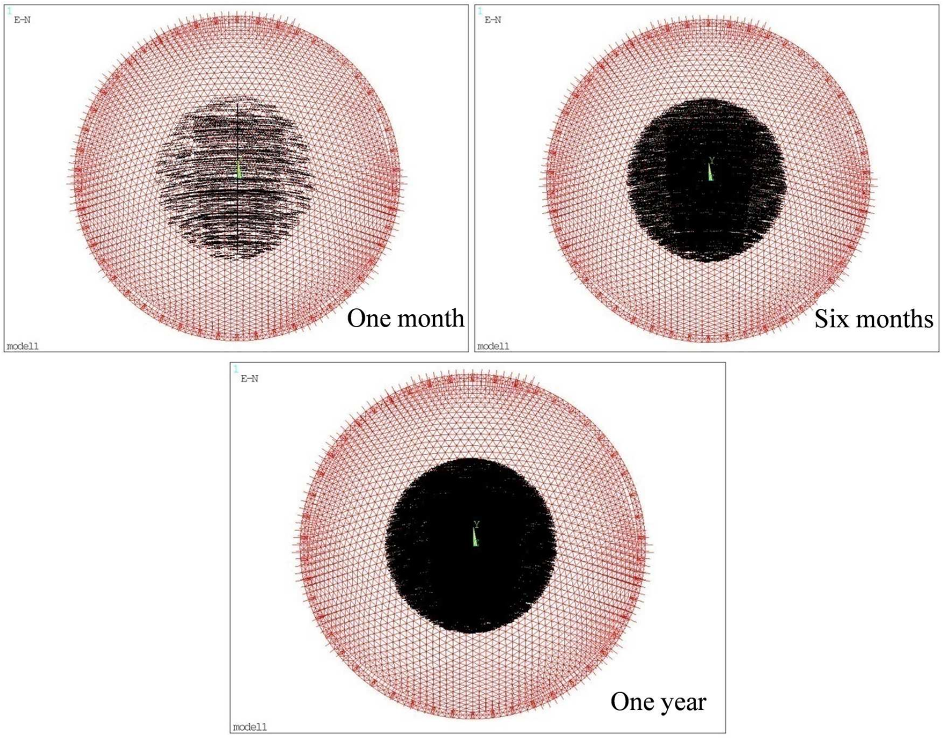

Fig. 6 Estimated trajectories of the parabolic center.

parabolic center to describe this problem, we can use MATLAB software to draw the observation trajectory over different time periods, as shown in Figure 6.

According to the design principle of the reflector system, the edge of the cable net is fixed on the ring beam. The illuminated region cannot extend beyond the 500-meter diameter, and the maximum observation zenith angle is 26.4 degrees. The trajectory of the illuminated aperture is thus limited to be within a certain region near the center of the reflector.

3.2 Estimation of Fatigue Cycles

It is unrealistic and unnecessary to use time history analysis to simulate the process of changing shape. Fortunately, this process in the FAST cable net can be simplified as a quasi-static process. We can thus simplify the continuous tracking process as a series of discrete deformation states.

We verified that any possible observation state is approximately equivalent to one of the 550 deformation states. Thus, with the above 3 410 008 tracking points, the stress-time curve for each cable can be estimated from the simulation results of the 550 deformation states.

Currently, the rain flow count method is the most commonly used method to analyze a fatigue stress spectrum (Kong et al. 2013; Fan et al. 2010). We can use this method to derive both the stress range and number of cycles. A program was thus written to apply the rain flow count method in processing the stress-time histories of all cables. The number of load cycles for each cable is thus derived.

The statistical results show that, in the above mentioned 228 715 observations, each cable went through between 840 107 and 1 020 054 cycles. The effect of the mean stress level is negligible when

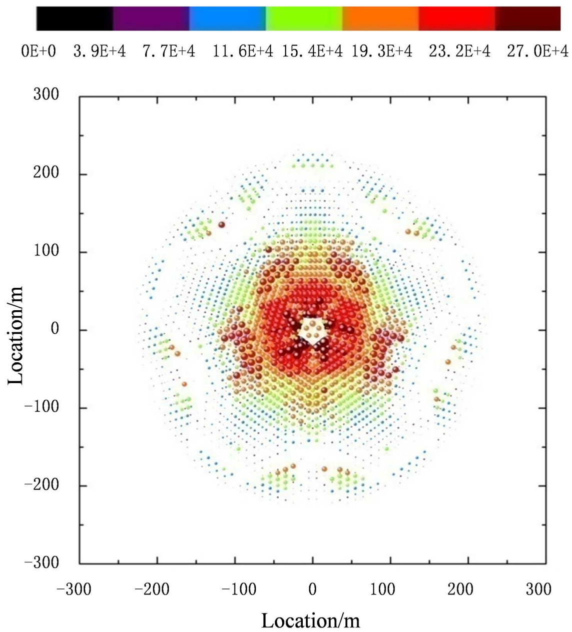

Fig. 7 Distribution of the stress cycles for a stress range exceeding 300 MPa.

the mean stress is between 15% and 40% of the ultimate tensile strength (Jeong & Sung 2000). Our cable strength design performs well in this situation, so the effect of the mean stress is thus ignored here.

In general, certain materials have a fatigue limit or endurance limit that represents a stress level below which the material does not fail and can be cycled infinitely. Therefore, fatigue cycles when cables are in a higher stress range are of more concern here, especially when the stress range exceeds 300 MPa. The distribution of the number of cycles when the stress range exceeds 300 MPa is plotted in Figure 7.

Figure 7 shows that the stress range exceeds 300 MPa for 270 027 cycles. There is obvious regularity in that there are more fatigue cycles in the process of changing shape closer to the center of the reflector. It is worth noting that the highest stress range and the maximum number of cycles are located near to one another.

By comparing the stress range and number of fatigue cycles of each cable, we can select a characteristic cable that we recognize as having a greater chance of failing to perform more detailed analysis. Figure 8 shows the statistical results of the number of cycles versus the stress range in the above mentioned 228 715 observations.

There are 1.8×10^5, 1.7×10^5 and 1.1×10^5 cycles for stress ranges of 200∼300, 300∼400 and 400∼455 MPa, respectively. There are approximately 4.6×10^5 fatigue cycles for which the stress range exceeds 200 MPa. Together with the stress range below 200 MPa, the number of cycles for this cable in total comes to 1.02×10^6 times.

4 FATIGUE EXPERIMENT

According to the above results from numerical analysis, the cable stress range generated by the process of changing shape is about twice the standard recommended value. The designed service life of FAST is 30 years. However, in accordance with international practice, such a large radio

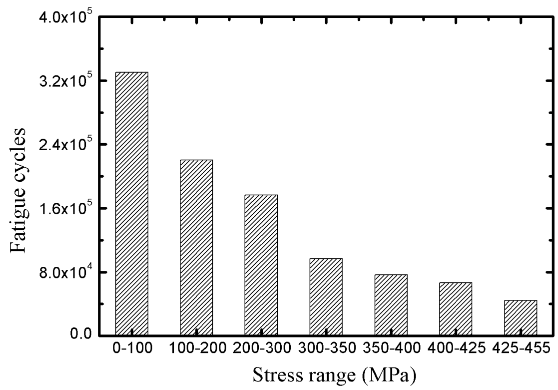

Fig. 8 Statistical result of the number of fatigue cycles versus the stress range.

telescope would in general be in service for at least 50 years. Arecibo, for example, has been in service for more than 50 years. Moreover, the trajectory path of the illuminated aperture on the spherical cable-net is difficult to estimate accurately.

For reasons of safety, the FAST project has proposed rigorous engineering requirements for the cables; i.e., the steel cables used in FAST construction should be able to endure 2×10^6 cycles of a fatigue test under a stress range of 500 MPa. This is a serious challenge for a steel cable, with no successful experience that can be used as a reference. Therefore, we start the present work from the basic tensile elements of the steel cable system; i.e., the steel wire and steel strand.

4.1 Steel Wire

Previous research (Birkemaier 1980) has shown that there is a direct relation between the fatigue resistance of a steel cable and that of its steel wire. It is necessary, especially in the case of the requirement for high fatigue resistance of FAST, to start an investigation by focusing on the steel wire that is the base material for the steel cable system. The Post-Tensioning Institute has specified that the minimum fatigue test strength/performance of a single steel wire should be 370 MPa under 2×10^6 load cycles.

In general, the fatigue strength of a steel cable system, because of fretting fatigue and the non-uniform stress distribution, is somewhat lower than that of steel wire. Therefore, the above mentioned fatigue strength of a single steel wire would be unable to satisfy the requirement of the cables that are used for FAST. Fortunately, improved materials have become available. We thus perform a fatigue test using the Chinese domestic supply of the latest high-performance steel wire.

Super 82B galvanized steel wire (1860-MPa grade), manufactured by Baoshan Iron and Steel Company, Ltd., is selected to carry out the fatigue test. In the test, the tensile load fluctuates according to a sinusoidal pattern with a constant amplitude, and the stress range is set at 600 MPa (from 144 to 744 MPa). The purpose of the redundant 100 MPa is to allow for a reduction in the fatigue strength after the cable system is manufactured from the steel wires. The specimen is 200 mm in length and 5.20 mm in diameter (see Fig. 9). The experiment loading frequency is 10 Hz.

The experimental results show that all six specimens endured 2×10^6 cycles in the fatigue test. We thus conclude that the fatigue strength of a single steel wire has obviously improved beyond the historical value given above. However, it should be noted that fretting fatigue between adjacent wires will obviously affect the fatigue resistance. Further experimental investigation of the steel strand is still needed.

Fig. 9 Photograph of the fatigue test conducted on a single Super 82B galvanized steel wire.

4.2 Steel Strand

The problem of fretting fatigue is the most important factor affecting the fatigue resistance of a steel strand or cable system. We thus have reason to believe that the type of coating on the steel wires will play an important role. Consequently, strands with different types of coating were tested in the present work, such as no coating, galvanized coating, and epoxy coating strands.

In general, epoxy-coated steel wire strands can be classified as filled epoxy-coated steel wire strands and individual epoxy-coated steel wire strands. The latter is selected in the present work mainly because its steel wires are individually isolated from each other by an epoxy coating, which efficiently reduces the stress concentration and friction damage on the surface of the steel wires.

All samples are in the form of 1×7 strands with a nominal diameter of 15.2 mm and length of 1000 mm. The stress range is conservatively set to 550 MPa, which is 50 MPa higher than our requirement for the steel cable system.

The tested strand was anchored by a wedge-type anchor, which is a common mechanism used for anchorage. The fatigue test was performed on an MTS hydraulic fatigue machine frame (see Fig. 10). To eliminate the uneven distribution of stress, the specimen was subjected to initial loading from zero to about 80% guaranteed ultimate tensile strength. Dynamic loading was then applied between 13.12% and 40% of the guaranteed ultimate tensile strength. The fatigue test was performed at a loading frequency of approximately 10 Hz. The results for different strands are listed in Table 2.

Table 2 Fatigue Test Results for Different Types of Steel Strands with a Wedge-type Anchor

Coating	Load range (kN)	Stress range (MPa)	Cycles
No coating	27.28–104.28	550	3.0×10^5
No coating	27.28–104.28	550	2.88×10^5
No coating	27.28–104.28	550	2.07×10^5
No coating	27.28–104.28	550	2.8×10^5
No coating	27.28–104.28	550	1.5×10^5
Galvanized coating	27.28–104.28	550	4.56×10^5
Galvanized coating	27.28–104.28	550	5.58×10^5
Epoxy coating	27.28–104.28	550	2.0×10^6
Epoxy coating	27.28–104.28	550	2.0×10^6
Epoxy coating	27.28–104.28	550	2.0×10^6

Fig. 10 Photograph of the fatigue test on a steel strand.

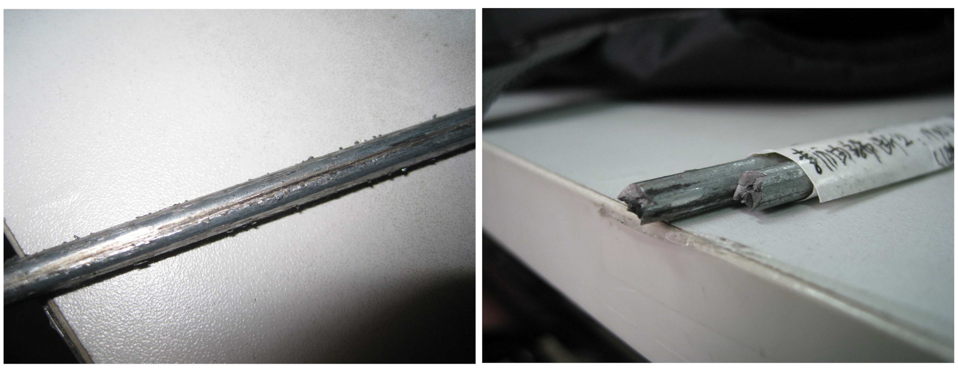

Fig. 11 Wear and scratching on the surface of a steel wire acquired from a steel strand broken in a fatigue test.

Table 2 shows that all six strand samples with no coating broke within 300 000 cycles, and the two galvanized strands both broke at about 500 000 cycles. The present test result revealed that the obvious reduction in fatigue resistance of these two types of strands, compared with the fatigue resistance of their steel wires, may result from fretting fatigue between adjacent wires. We then took a steel wire from one broken strand sample to observe the friction at its surface.

Figure 11 shows an obvious scratch on the surface of this steel wire. Under repeated fatigue loadings, such scratches are most likely to be the sources of initial cracks, and thus reduce the fatigue strength of the steel strand.

In the case of an individual epoxy-coated steel wire strand, the stress concentration and friction damage on the steel wire surface are efficiently reduced by the epoxy coating between the steel

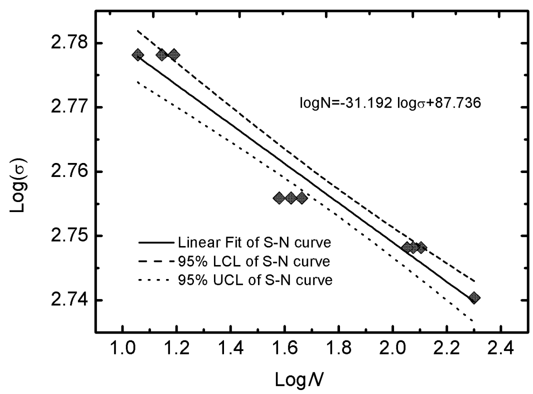

Fig. 12 Linear regression of log ($\Delta\sigma$) versus log (N) obtained in our experiment on the epoxy-coated strand.

wires. Therefore, this type of strand was found to have high fatigue resistance. In our test, all three samples of this type of strand endured 2×10^6 fatigue cycles under a stress range of 550 MPa.

4.3 S-N Curve

The cable-net structure is the most critical and fragile part of the FAST reflector system, and the service life of FAST directly depends on the residual fatigue life of the structure. FAST has a designed life of 30 years, and it is necessary to develop a fatigue damage monitoring system for such an important facility.

The S-N curve plots the basic data used in the evaluation of the structural fatigue life. However, it would be highly impractical and expensive to perform stay cable system fatigue tests at various numbers of load cycles and stress ranges to establish S-N curves. Fortunately, a significant amount of experience has verified that the performance of an individual prestressing element, anchored with the actual anchorage mechanism of the stay cable system, can be used as an indication of the approximate performance of the stay cable system (see footnote 2).

Therefore, fatigue tests for different stress ranges were performed on epoxy coated steel strands. Here, the upper stress was fixed at 744 MPa, and different stress ranges of 550, 560, 570, 580 and 600 MPa were applied by changing the lower stress. Three samples were tested for each case.

The test results reveal that the fatigue life of a strand obviously declines with an increase in the stress range. At a stress range of 600 MPa, strands generally broke after approximately 150 000 cycles. At a stress range of 580 MPa, the three samples broke between 320 000 and 460 000 cycles. At a stress range of 560 MPa, the three samples broke between 1 130 000 and 1 270 000 cycles. The relationship between the applied stress range and fatigue life can be plotted using dual logarithm coordinates as shown in Figure 12. Employing the least-squares method, the S-N curve of the type of strand investigated can be derived as

$$\log(N) = 87.736 - 31.192 \cdot \log(\Delta\sigma)\,, \tag{9}$$

where $\Delta\sigma$ is stress range and N is the number of fatigue test cycles.

Fig. 13 Photograph of the location of the cable test.

4.4 Cable System

For stay cable systems to achieve the specified minimum test performance requirements, the stay cable anchorage systems need to be carefully designed and detailed. In this work, traditional extruding anchoring technology was improved by adding a layer of cushioning material between the cable and anchoring device, and the anchoring system of the cable was manufactured by internal squeezing.

Employing the improved anchoring, $3 \times \Phi 15.2$ and $6 \times \Phi 15.2$ cables, having effective cross-sectional areas of 420 and 840 mm^2 respectively, were fabricated. The cross sections of tested cables were selected by referring to the actual cross section selection used in the FAST cable-net structure. Tests were carried out at the Supervision and Test Center for Product Quality, administered by the Ministry of Railways and the Chinese Railway Bridge Bureau Group Corporation. Figure 13 shows a tested cable.

According to the requirements of the standards, the free segment length of the six cables was 3 m. To eliminate the uneven distribution of stress, the specimen was subjected to an initial loading from zero to about 80% of the guaranteed ultimate tensile strength. The fatigue tests were performed under a fatigue stress amplitude of 500 MPa, maximum stress of 744 MPa and loading frequency of 3 Hz. The number of fatigue loadings reached 2 million without failure. Table 3 gives the experimental results for the six cables.

Table 3 Experimental Results for Cables

Cable specifications	Stress amplitude	Number of cycles	Location
$3 \times \Phi 15.2$	500 MPa	2 million times	Ministry of Railways
$3 \times \Phi 15.2$	500 MPa	2 million times	Supervision and Test Center
$3 \times \Phi 15.2$	500 MPa	2 million times	for Product Quality
$6 \times \Phi 15.2$	500 MPa	2 million times	Chinese Railway Bridge
$6 \times \Phi 15.2$	500 MPa	2 million times	Bureau Group Corporation
$6 \times \Phi 15.2$	500 MPa	2 million times	

5 CONCLUSIONS

During FAST observations, the stress range generated by the process of changing shape is more than twice the standard recommended value. To improve the reliability and service life of FAST, we carried out an extensive numerical and experimental investigation. The following conclusions are drawn from the results of the investigation.

(1) The focal ratio is the key influencing factor for the stress range of the FAST cable-net structure generated by the process of changing shape. Additionally, a focal ratio of 0.4621 is suggested as most appropriate, leading to a reduction in the stress range of approximately 30 MPa and a reduction in the actuator stroke of 50 mm.
(2) The tracking trajectory was planned according to the demands of the scientific objectives of FAST during its service life of 30 years. The technical requirements of the cables were obtained by mathematically simulating the tracking trajectory of FAST.
(3) Compared with the historical value, there was an obvious improvement in the fatigue performance of a steel wire. In our fatigue test on the Super 82B steel wire, all six samples endured 2×10^6 cycles under a stress range of 600 MPa.
(4) Because of fretting fatigue, different types of coating on the steel wire surface can obviously affect the fatigue performance of the strand. In our experiments on three types of coating strands, the best performance was found for the individual epoxy-coated steel wire strand, with all three samples enduring 2×10^6 fatigue cycles under a stress range of 550 MPa.
(5) S-N curves of the individual epoxy-coated steel wire strands were derived, giving basic data for the evaluation of the fatigue life of the FAST cable net in future operation.
(6) The steel cable system was subjected to fatigue tests under a stress range of 500 MPa for 2 million fatigue loadings. We thus developed a steel cable system that could operate under high stress amplitude that was targeted at the relevant technical engineering requirements of FAST.

Acknowledgements This work was supported by the Young Scientist Project of the National Natural Science Foundation of China (Grant No. 11303059) and the Chinese Academy of Sciences Youth Innovation Promotion Association. We would like to thank all our colleagues for their contributions to our study.

References

Barenblatt, G. I. 1996, Scaling, Self-similarity, and Intermediate Asymptotics (Cambridge: Cambridge Univ. Press)
Birkemaier, M. 1980, in IABSE Proceedings, 30
Fan, F., Jin, X. F., & Qian, H. L. 2010, Journal of Building Structures, 31, 17
Jeong, I. S., & Sung, P. C. 2000, International Journal of Fatigue, 22, 339
Jiang, P., Wang, Q. M., & Zhao, Q. 2013, Engineering Mechanics, 30(2), 400
Kong, X., Jiang, P., & Wang, Q. M. 2013, Engineering Mechanics, 30(s), 169
Lu, Y. J., & Ren, G. X. 2007, Engineering Mechanics, 24, 165
Luo, Y. F., Yang, W., Li, G. Q., et al. 2004, Structural Engineers, 30
Nan, R., Li, D., Jin, C., et al. 2011, International Journal of Modern Physics D, 20, 989
Nan, R., Ren, G., Zhu, W., & Lu, Y. 2003, Acta Astronomica Sinica, 44, 13
Qian, H. L., Fan, F., Shen, S. Z., et al. 2005, China Civil Engineering Journal, 38, 18